Journal of Manufacturing Systems 80 (2025) 356–365

Contents lists available at ScienceDirect

Journal of Manufacturing Systems

journal homepage: www.elsevier.com/locate/jmansys

Technical paper

Life cycle assessment and energy characterization of friction surfacing deposition of aluminum alloys

Simone Amantia [a], Kirill Kalashnikov [a], Gianni Campatelli [b], Livan Fratini [a], Giuseppe Ingarao [a,*]

[a] Department of Engineering, University of Palermo, Viale delle Scienze, Palermo 90128, Italy
[b] Department of Industrial Engineering, University of Florence, Via di Santa Marta 3, Firenze 50139, Italy

ARTICLE INFO

Keywords:
Additive manufacturing
Friction surfacing
Wire arc additive manufacturing
Life Cycle Assessment
Environmental Impact

ABSTRACT

In this work, an experimental investigation of Friction Surfacing Deposition (FSD) using the 2000-series heat-treatable aluminum alloy was performed including the environmental impact characterization of the process. The effect of main controlling process parameters and their interactions on energy demand during the single layer deposition was evaluated. A full Life Cycle Assessment (LCA) analysis was conducted for layer-by-layer deposition and a comparison of FSD with the Cold Metal Transfer Wire Arc Additive Manufacturing (WAAM) was performed for a specific wall-shaped sample production. It was observed that the FSD process is characterized by lower processing energy than WAAM, but also by a much higher amount of material scrap connected to undeposited parts of consumable tools such as a flash. To assess the possibility of reducing the material waste during FSD, the comparative LCA analysis was expanded to study the impact of the deposited layer length. It was shown that the FSD method can be a more environmentally friendly process when the deposition of at least 450-mm-long layer using a unique tool is required.

1. Introduction

Nowadays, the production of large-sized components is one of the most challenging tasks for metal additive manufacturing (AM) [1]. Production of turbine blades, fuel tanks, thrust chambers, and other parts of aircraft and spacecrafts using conventional manufacturing is a high-cost, multistep process, and the application of additive manufacturing can improve the leading time as well the environmental and economic impact [2–4]. The most studied and most frequently used technologies of powder-bed selective fusion of metallic materials are not suitable for this case because of their slow deposition rate and strong requirements to the storage and handling of the feedstock material, in addition to the limited working space for manufacturing [5,6]. To avoid these problems, methods of Directed Energy Deposition (DED) have been developed [7]. Such methods include powder- or wire-based laser-beam DED, electron beam freeform fabrication, and Wire-Arc Additive Manufacturing (WAAM) [8–10]. Powder-based laser-beam DED has advantages such as high accuracy and flexibility of the process, but it still operates with powder, making this process more difficult for large-scale manufacturing, while it is well suited for part repairing. In contrast, wire-based DED can work with any commercial or other filament and provides about 6 times higher deposition rate, making these processes easy to implement in comparison to powder-based technologies [11]. At the same time, some of these methods require expensive heat sources and a special atmosphere, such as a vacuum for electron beam. In this way, the wire-arc process becomes simpler to implement because it is based on the most used welding techniques [12]. More than that, in recent years, some researchers and engineers have been working on adapting WAAM for aluminum alloys using the Cold Metal Transfer (CMT) approach [13,14]. This method is characterized by much lower heat inputs than standard WAAM, thanks to the joint action of a pulsed arc and mechanical pull of the material into the melting pool that reduce the current required for the detachment of the drop of melted material from the consumable wire. The use of CMT impacts also the quality of the deposition, since without CMT, standard WAAM relates to high porosity of aluminum alloys, cracking, distortion, and shape irregularities because of welding bead geometry [10]. Especially, CMT is beneficial for heat-treatable aluminum alloys which have a limited weldability. There are already some positive results on the CMT-WAAM using AA2319 commercial wire [15,16]. For example, Pan et al. [16] produced wall-shaped samples up to 8 cm in height. They reported no

* Corresponding author.
E-mail address: giuseppe.ingarao@unipa.it (G. Ingarao).

https://doi.org/10.1016/j.jmsy.2025.03.008
Received 12 March 2025; Accepted 14 March 2025
Available online 24 March 2025

Nomenclature

AM	Additive manufacturing
AFSD	Additive friction stir deposition
ASIHM	Additive-Subtractive Integrated Hybrid Manufacturing
CED	Cumulative Energy Demand
CMT	Cold Metal Transfer
CNC	Computer numerical control
DED	Directed Energy Deposition
DMLS	Direct Metal Laser Sintering
DR	Deposition Rate
FSD	Friction Surfacing Deposition
FSW	Friction Stir Welding
GWP	Global Warming Potential
LPBF	Laser Powder Bed Fusion
LCA	Life Cycle Assessment
PP	Production phase
PMC	Pulse multi control
R	Recycle Content
SEC	Specific Energy Consumption
TRL	Technology Readiness Level
WAAM	Wire Arc Additive Manufacturing

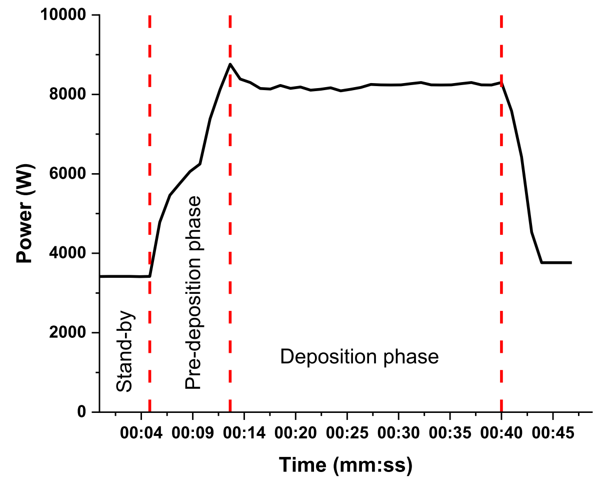

Fig. 2. Electric power trend of FSD Process during a single layer deposition.

hot cracking behavior, while there is still a porosity observed in each deposited layer, so this process requires further studies to eliminate remaining defects.

Meanwhile, there is another promising group of processes suitable for large-scale additive manufacturing working on principles of solid bonding [17]. This group is called friction-based additive manufacturing, and methods included in this group originated from Friction Stir Welding (FSW), which is well suited for lightweight alloys having problems with conventional welding techniques [18,19]. This problem is mostly connected to heat-treatable alloys of the 2000 series which have poor weldability and printability by fusion-based methods [20]. In [20], there was an attempt to build an additive sample made of AA2024 alloy using laser powder-bed AM, indicating problems with hot cracking on grain boundaries. On the other hand, friction stir welded AA2024 alloy does not experience temperatures higher than 0.8 of the melting point, avoiding cracking and porosity [21]. Inside the group of friction-based AM, there are methods of Additive Friction Stir Deposition (AFSD) and Friction Surfacing Deposition (FSD), both of which are performed using consumable tools (mechtrodes) as a feedstock [22,23]. The AFSD method has some advantages in comparison with FSD because of using a stationary shoulder to avoid some tool deformation features

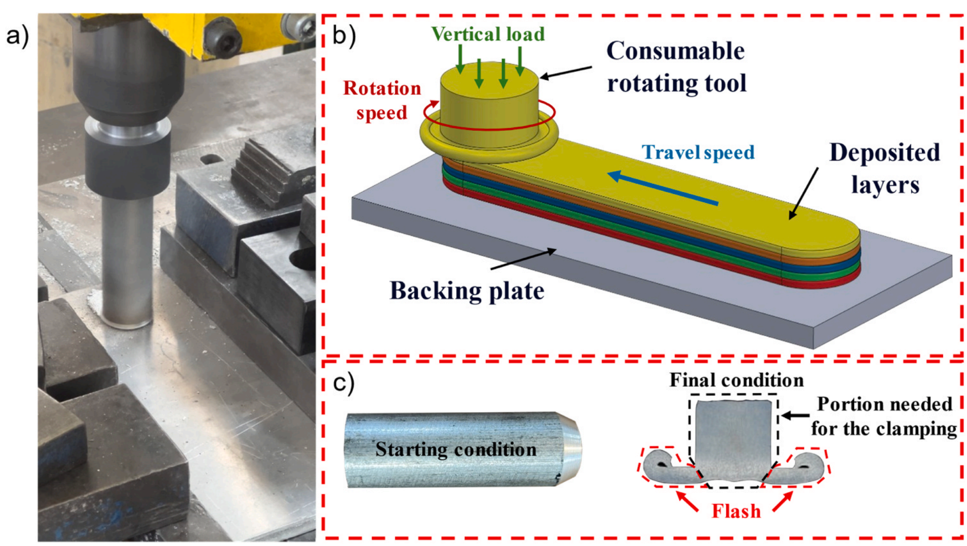

Fig. 1. Friction Stir Deposition experimental set-up (a) and a schematic illustration of the process (b) along with the starting and final conditions of the consumable tool (c).

Table 1
The developed experimental campaign.

ID	F [kN]	V [m/min]	ω [rpm]	t_{PP} [s]	DR [g/s]	P [kW]	E_{tot} [kJ]	SEC [kWh/kg]
1	6	0.3	800	40	0.80	6.8	278	3.2
2	10	0.3	800	40	1.17	8.1	324	2.4
3	6	0.5	800	24	0.60	8.2	186	5.7
4	6	0.3	1400	40	0.49	7.0	290	6.7
5	10	0.5	800	24	1.75	7.1	174	1.4
6	10	0.3	1400	40	0.31	7.7	312	6.7
7	6	0.5	1400	24	0.54	7.7	190	4.1
8	10	0.5	1400	24	0.62	7.4	182	3.9

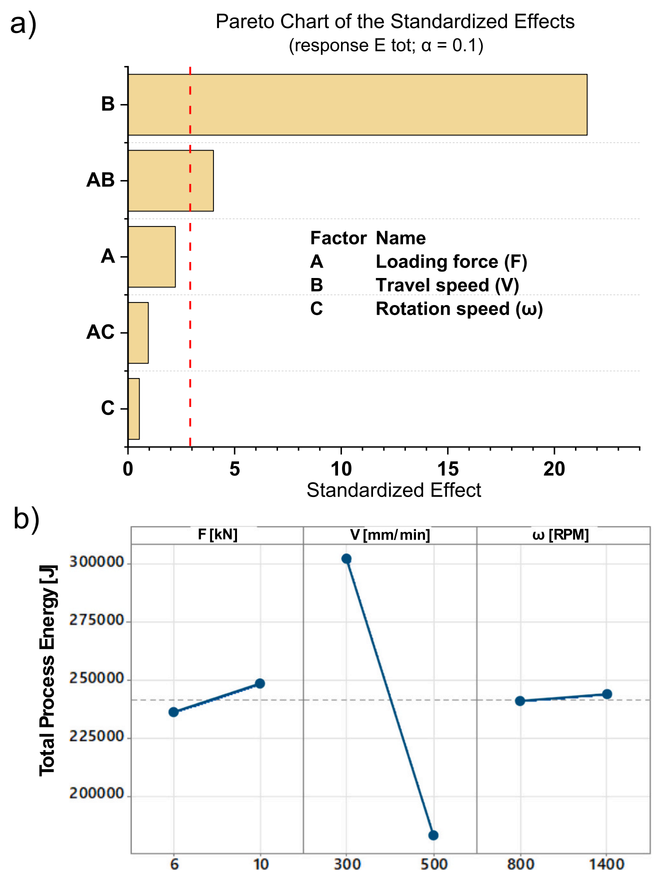

Fig. 3. Pareto chart (a) and main effect plots (b) for the FSD process, showing the influence of process parameters on the total energy used for the deposition of a single layer.

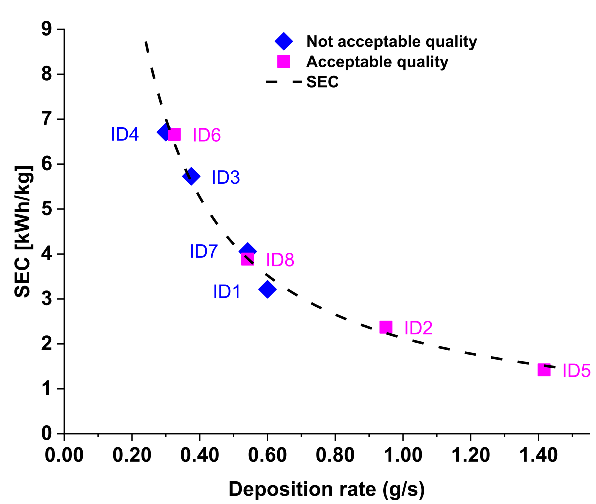

Fig. 4. SEC trend with varying deposition rate.

such as flash formation [24]. However, the application of such an approach requires specially designed equipment to implement an additional axis for rod feeding. For example, the MELD company has patented its own AFSD technology and sells specialized machines for its implementation [25]. On the other hand, the FSD method has no such restrictions and can be easily conducted on different kinds of machines, starting with Computer Numerical Control-milling (CNC) ones and ending with robotic friction stir welding machines [26]. As an alternative to DED methods, FSD can allow the production of thick walls with a

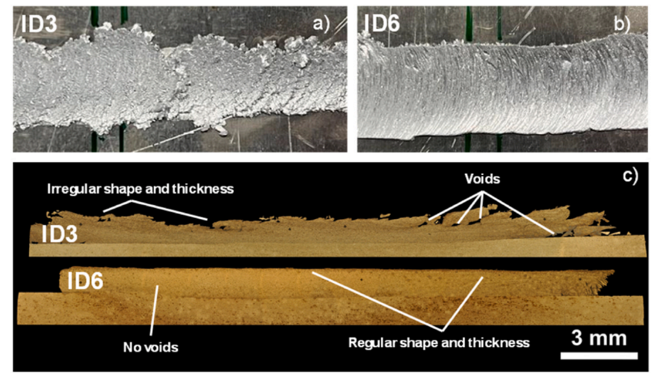

Fig. 5. Deposition quality of ID3 (a) and ID6 (b) parameter sets in top view and their cross-section view (c).

high deposition rate because the width of the layer depends on the consumable tool diameter [27]. There are several papers on FSD of different aluminum alloys, including heat-treatable ones, showing good suitability of this method for additive manufacturing using these materials in comparison to fusion-based techniques [28–30]. For example, Antunes Duda et al. [28], produced dissimilar FSD samples using deformable AA5083 and heat-treatable AA2024 alloys. Soujon et al. [29] have shown that using FSD it is possible to achieve the deposit width of 30 mm just by two overlapping passes by a 20-mm-diameter consumable tool, illustrating the strong applicability for large-scale AM. However, despite high deposition rates, this method is facing problems with material waste. There are two reasons for that. First, consumable tools used for the deposition usually utilize a maximum of about 1/3 of their volume depending on the production mode and cannot be used as a tool again because of the flash formation and heat effect leading to changes in mechanical properties of parent material. Consequently, they must be subjected to recycling to produce new rods. Second, as-built components have shape irregularities and/or defects which should be removed by milling processing, resulting in a high amount of process scrap to obtain a final shape [31]. In this way, it is necessary to understand if FSD technology is at least comparable with already used technologies such as WAAM in terms of material costs and energy efficiency.

Researchers' interest in the environmental impact of metal additive manufacturing processes has grown in recent years [32,33]. Several LCA models have been developed for additive manufacturing processes [34,35]. Kokare et al. [36] developed a model to evaluate and compare the environmental impact incurred during the manufacture of a given product using WAAM, Laser Powder Bed Fusion (LPBF), and pure CNC machining methods. From this study, WAAM stands out as a more sustainable and cost-effective option, particularly for larger parts, due to its superior material efficiency compared to CNC milling and higher deposition rate when compared to LPBF. Liu et al. [37] performed a comparative analysis of additive-subtractive integrated hybrid manufacturing (ASIHM), which integrates laser directed energy deposition with CNC milling, against conventional subtractive manufacturing to produce thin-walled titanium components. In the ASIHM process, the laser and chiller are the primary sources of energy consumption within the additive system, contributing to approximately two-thirds of the total carbon emissions. Colombini et al. [38] investigated the balance between mass reduction and productivity in assessing the environmental sustainability of lattice structures manufactured via LPBF. Using a Life Cycle Assessment, they compared two design variants of an automotive component: a topologically optimized version featuring a solid bulk section and an alternative design with lattice structures aimed at further weight reduction. Their analysis indicated that most emissions identified in the midpoint assessment were predominantly due to the substantial power consumption throughout the

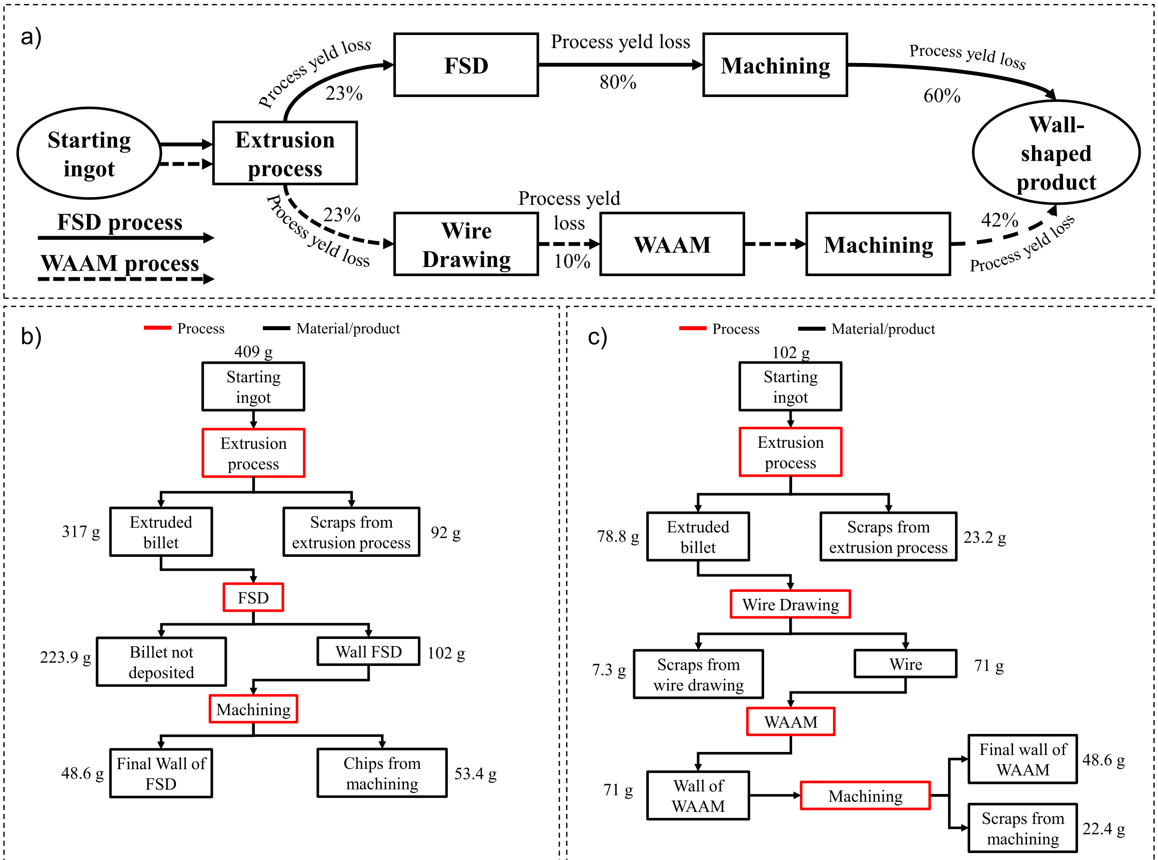

Fig. 6. System boundaries of FSD and CMT-WAAM processes (a); mass flow study results of FSD route (b) and WAAM route (c).

Table 2
Life cycle inventories for CMT-WAAM.

Energy of single-dot deposition process (kJ)	2.21
SEC (MJ/kg)	8.72
Shielding gas consumption for single drop deposition (l)	0.435

process. Reis et al. [39] conducted an applied study involving the production of three metal parts with varying levels of complexity, comparing an additive manufacturing process (WAAM) and a subtractive process (CNC-milling). To assess the environmental impacts of each approach, the Life Cycle Assessment (LCA) methodology was employed. The findings enable a comparative analysis of the two manufacturing methods and provide insights into potential strategies for reducing WAAM's environmental impact. Their results reveal that the WAAM process achieves material savings of 40 % to 70 % and reduces environmental impact by 12 % to 47 % compared to the subtractive approach for the three geometries examined in this study. Bekker and Verlinden [40] evaluate the environmental impact of WAAM in contrast to conventional manufacturing methods for stainless steel components, specifically green sand casting and CNC milling. It was shown that a major contribution (from 15 % to 30 %) to total impact relates to the deposition stage in terms of employed electricity and shielding gas consumption. Kokare et al. [41], through a cradle-to-gate analysis, reports that inert gas contributes at least 12 % to the total environmental impact of WAAM in the case of steel. At the same time, the impact of shielding gas consumption while WAAM of aluminum alloys remains not evaluated yet.

Friction-based additive technologies, in turn, are less studied than WAAM and other methods from the environmental impact point of view. Ahmed et al. [42] performed a comparative sustainability assessment between AFSD (by MELD process) and Direct Metal Laser Sintering (DMLS) techniques. The study results indicate that AFSD demonstrates higher sustainability performance, reaching a sustainability score of 69 % compared to DMLS, which scores 31 %. The sensitivity analysis highlights that differences in build volume between the two processes have the most pronounced impact on the sustainability score, contributing to a 4.2 % variance.

In conclusion, friction-based additive manufacturing approaches are a quite new process category that can be considered an alternative to more conventional DED processes such as WAAM or Laser/EBM-based approaches. Drawing on high deposition rates and ability to use aircraft aluminum alloys (AA2XXX), both FSD and WAAM processes can be used for large-sized aerospace components production [43,44]. Nevertheless, the environmental performance of this process category is still to be characterized, as the literature review shows a lack of analysis from this angle.

This work aims at filling this research gap and proposes energy characterization and Life Cycle Assessment analysis of Friction Surfacing Deposition of 2000 series heat-treatable aluminum alloys. Additionally, because CMT-WAAM can also perform additive manufacturing of large-sized products made of heat-treatable aluminum alloys, it is interesting to compare FSD and WAAM to identify the most appropriate use cases for a particular technology considering their environmental impact.

2. Materials and methods

In the present study, an electrical energy characterization of FSD process and a LCA comparative analysis, between FSD and WAAM is developed. For the LCA analysis all the energy and resource flows were analyzed for the manufacturing of vertical wall made of 2000 series aluminum alloy.

For the FSD process, the effect of process parameters on the energy

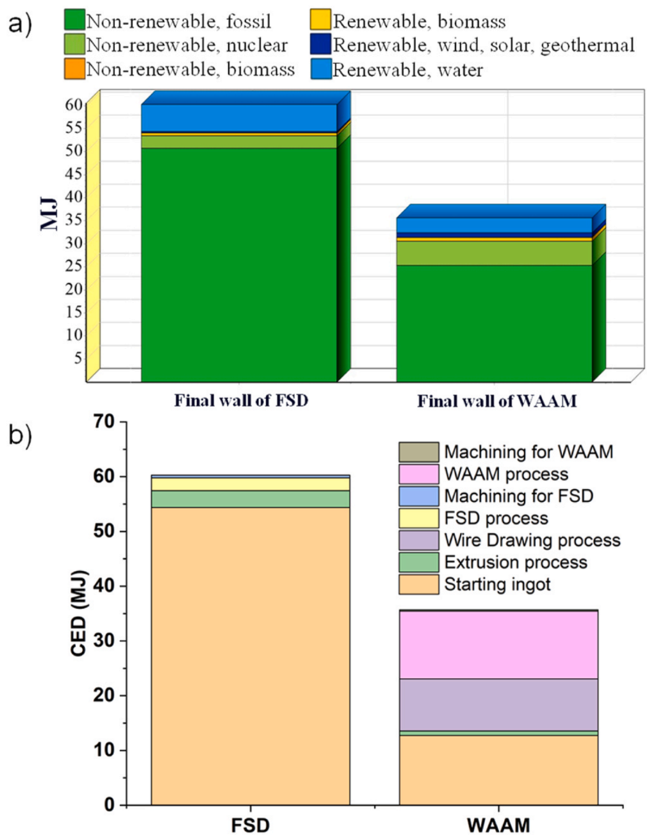

Fig. 7. CED results (a) and related breakdown analysis (b).

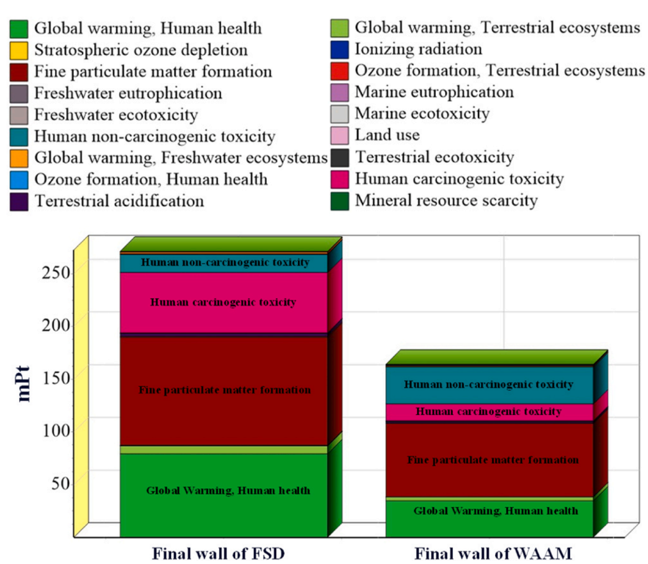

Fig. 8. LCA results with Endpoint ReCiPe2016 (H) method (mPt) for impact category.

absorbed by the used machine was analyzed. Additionally, the Specific Energy Consumption (SEC) curve and its corresponding equation as a function of the deposition rate (g/s) were derived. The developed experimental campaign is reported in Sections 2.1 and 2.2.

2.1. FSD Process

Friction Surfacing Deposition has been performed using a dedicated Friction Stir Welding machine, ESAB Legio 3ST (ESAB Corporation, Gothenburg, Sweden). As the feedstock material, rods with a diameter of 25 mm made of AA2011 heat-treatable aluminum alloy were used (Fig. 1).

A chamfer of 5 mm was added to the rods' design to improve the pre-deformation stage.

The deposition process was conducted as follows. The consumable tool was fixed in the welding head using the specially developed screwing system, and the 3-mm-thick AA2011 substrate was placed on the working table and mechanically clamped as shown in Fig. 1. Then, under the force-controlled mode, after reaching the target vertical load $\boldsymbol{F}$ during the pre-deformation stage, the tool started to move along the line with specific travel $\boldsymbol{V}$ and rotation $\boldsymbol{\omega}$ speeds, creating the deposit layer. After each deposition, it is necessary to replace the consumed tool with a new one, and during this procedure, the machine is working in stand-by mode.

For energy characterization purposes, an experimental campaign based on the full-factorial experimental design was conducted. For this reason, 8 combinations of process parameters have been selected based on preliminary testing to produce 200-mm-long deposits. All the analyzed process parameters combinations are reported in Table 1. The weight of each deposit as well as each consumable tool after the FSD process was measured to assess the deposition rate. During the deposition process, the electrical energy used by the FSW machine was measured by means of a power and energy quality analyzer, Chauvin Arnoux C.A 8331 (sampling rate of 12.8 kHz, results logged and shown are for averaged values over 1 second intervals) connected to the machine input. Additionally, for LCA purposes, the multi-layered sample has been produced consisting of 5 layers with a target length of 125 mm. Then it was machined using the Mazak NEXUS 410A-II Vertical Machining Center (Yamazaki Mazak Corporation, Oguchi, Japan) to obtain a final shape of the vertical wall.

A typical power trend for one layer deposition is reported in Fig. 2, where the main production modes are highlighted. It is worth mentioning that the pre-deposition phase time includes the time for the target value force to be reached plus the time for reaching the proper starting temperature for initializing the material deposition.

To assess the acceptability of the quality of deposits produced by various FSD modes, the visual control method was used for analyzing external defects, as well as the metallography analysis was used to assess the bonding quality and internal defects. For this purpose, each deposit was cut out in the cross-section and prepared by mechanical grinding using different grit-size papers followed by polishing using diamond suspensions up to 1.0 μm grit-size. Polished surfaces were etched using Keller's reagent by 10 s immersion and then analyzed using an optical microscope, Olympus GX51 (Olympus Inc., Tokyo, Japan).

2.2. WAAM process for comparative analysis

To conduct comparative analysis, Wire-Arc Additive Manufacturing process using aluminum alloy wire has also been performed. The deposition was carried out using a Fronius TPS 320i power source with a CMT drive unit integrated into a robotic TPS/i setup (Fronius GmbH, Wels, Austria). To minimize heat inputs during the deposition, in addition to the CMT drive, the Cycle Step welding approach was used, it allows to perform a specific number of CMT cycles to create a single dot of material.

To deposit a material like the AA2319 it is required to maintain a low heat input and assure a cooling time for the deposited layers, thus avoiding over melting. The approach adopted to produce a wall-shaped part compliant with these requirements, a dot-by-dot deposition technique. For specific geometry and material, some preliminary tests have been carried out and the optimal deposition parameters, allowing to achieve a good quality of the part and productivity, consisted of 30 CMT cycles (yielding ~0.7 s of active deposition) followed by a dwell time of 2 s between the dots.

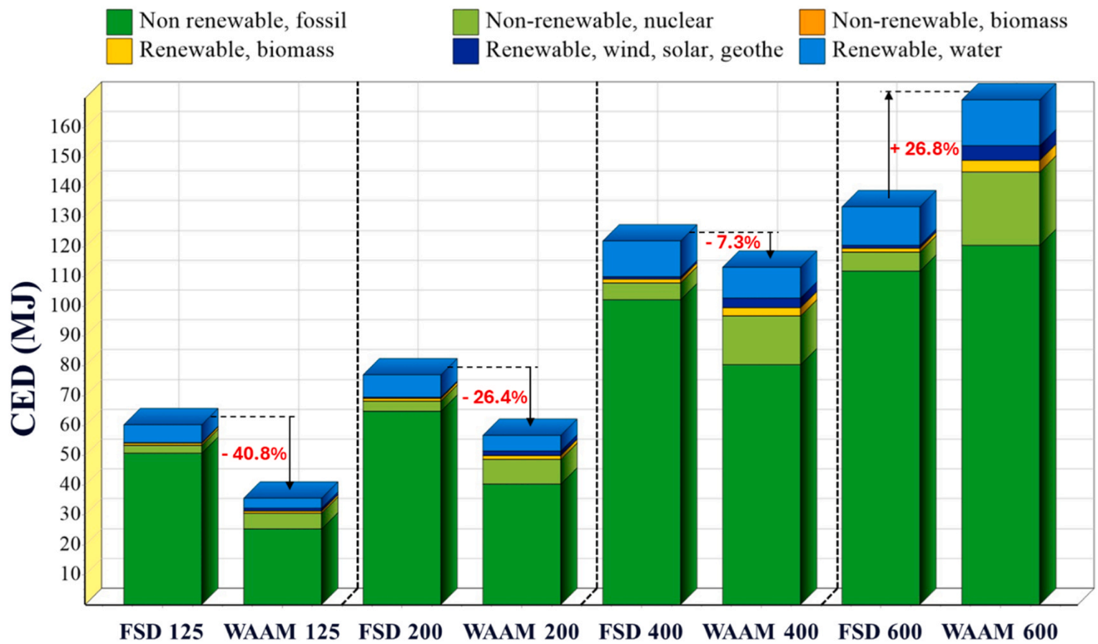

Fig. 9. CED results for different layer deposition lengths.

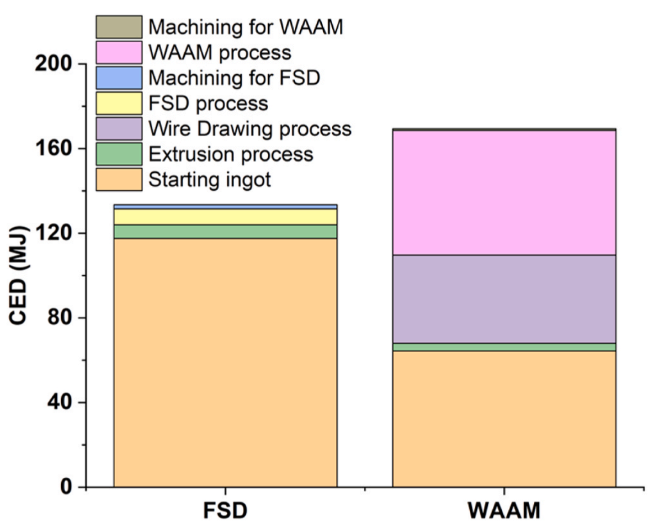

Fig. 10. CED breakdown results for 600 mm of deposition length.

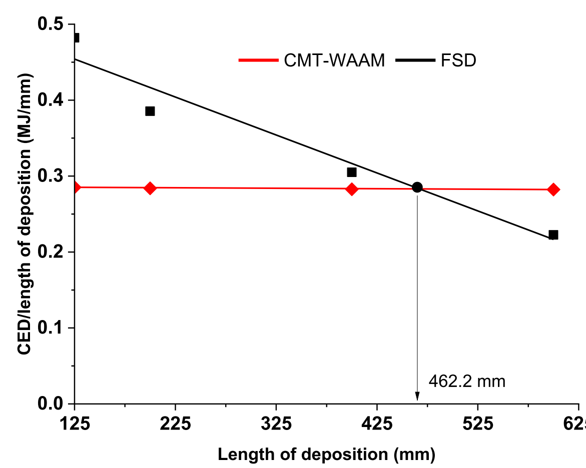

Fig. 11. Breakeven analysis for FSD and CMT-WAAM processes.

The test geometry produced with this approach is a 105-mm-long layer deposition, practically reducing stand-by energy consumption of both the power source and positioning system. To print the sample with the same size as the FSD one, the CMT-WAAM sample included two layers in width and 13 layers in height. A commercial AA2319 welding wire with a diameter of 1.2 mm was selected as feedstock to provide a comparison of heat-treatable alloy deposition methods. The deposition procedure was performed under shielding atmosphere (grade 5 high-purity argon gas). The process parameters used for the deposition are a current of 169 A, a voltage of 16.5 V, with a generator power of 3133 W, and a wire feeding rate of 6.7 m/min. This set of parameters allowed for a single-dot deposition volume of 89.2 mm^3.

The electrical energy absorbed by the WAAM system was recorded using a high-frequency data logger embedded in the power source, the machining of the final wall-shaped sample was performed using the Mazak NEXUS 410A-II Vertical Machining Centre. Along with electrical energy, shielding gas consumption and process scrap were included in the analysis as detailed in Section 4.3.

3. Effect of process parameters on energy demand

According to the full-factorial experimental design, 8 FSD deposits were produced using various combinations of process parameters (Table 1).

It was found that all the process parameters configurations allow layer formation, that is, enough level of solid bonding between the coating and the substrate. So, all the samples can be considered for analysis. The power-time data was recorded during the deposition for each parameter set. By means of the direct numerical integration method, the energy consumption for all the process parameter combinations was calculated using the power-time graphs like that shown in Fig. 2.

It is visible from Table 1 that the parameter choice affects the maximum power of the manufacturing stage. Using both minimal and maximum force and travel speed values along with the minimum rotation rate, the lowest energy level has been recorded with the value of about 6.8 – 7.1 kW. At the same time, using other process parameters configurations (ID3) the power grows up to 8.2 kW. At the highest value of rotation speed, the average power level is slightly lower (7.7 kW),

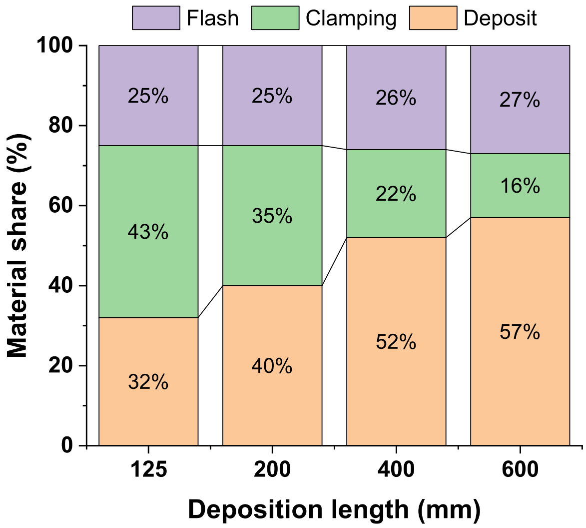

Fig. 12. Material shares in FSD for different deposition lengths demonstrating the fraction of scraps in total tool material utilization.

while the overall picture is the same as in the previous case.

The total energy was calculated, and Pareto analysis has been performed to understand which of the parameters has an influence on the energy consumption during the FSD process (Fig. 3).

Results of the analysis show that, as expected, the most significant effect on the total energy is the travel speed because of reducing the lead time. However, also the interaction of travel speed with force has a sufficient influence, while the effect is opposite.

Since the manufacturing process can include several layer depositions, and it can vary from one component to another, it is reasonable to represent the energy as the value necessary to perform the deposition of one unit of material. For this reason, SEC was calculated using the weight measurement data. Meanwhile, the efficiency of the production modes was assessed by the deposition rate (DR) considering the duration of the coating process and the weight of each sample. In Fig. 4, changes in the SEC are shown depending on the deposition rate. It is clear from the figure that with the increase in the deposition rate, energy consumption decreases.

The experimental data are effectively fitted by a curve expressed in the form of Eq. (1), which distinctly resembles the law commonly used to describe the SEC in metal cutting processes as the material removal rate varies.

$$SEC_{FSD} = 0.04 + \frac{2.09}{Deposition\ Rate(g/s)} \tag{1}$$

The SEC trend and related equation of fitting curve clearly resemble the laws that usually describe the SEC with varying the production rate. Kara and Li [45], Baffari et al. [46] and Lunetto et al. [47] found similar trends for machining, Friction stir extrusion and Fused Deposition Modeling, respectively.

This kind of relation is typical of the processes where energy consumption is primarily time-dependent, where the decrease in processing time effectively dominates over the possible increase in power demand. It is worth mentioning that the depicted trend of Fig. 4 is valid only for the set-up used in this research (deposited material, used machine and consumable rotating tool geometry).

There are some points characterized by the close values of SEC and DR (ID4 and ID6, ID7 and ID8 in Fig. 4). In order to reveal the difference between these modes as well as to understand the approximate process window in terms of SEC, the assessment of quality acceptability was performed (Fig. 5). It was found that samples ID3, ID4, and ID7 are not acceptable because of shape irregularities and other external defects as shown in Fig. 5, a. At the same time, samples ID1 and ID3 have coarse internal defects requiring extensive machining, making them also not acceptable (Fig. 5, c).

It must be noted that the difference of samples ID6 and ID8 from ID3 and ID7 is in the higher loading force value. It makes it possible to conclude that the increase in loading force can improve the material flow, leading to better top surface and minimal level of edge defects.

The developed experimental campaign allowed quantification of the material quantities and energy demand required to create a process model within the SimaPro software. Finally, ID5 process parameters configuration was chosen for the additive manufacturing purpose because of the minimum SEC value.

4. LCA framework

This section presents the LCA methodology used in the study, including the definition of the goal and scope, functional unit, system boundaries, and life cycle inventory analysis for the two separate processes. The interpretation of the LCA results is subsequently provided in Section 4.4. The study follows the ISO 14040/44 standards and ILCD guidelines [48], [49,50]. The analysis comprises a mid-point evaluation focused on Global Warming Potential (GWP) and Cumulative Energy Demand (CED), along with an end-point assessment of impacts on human health and ecosystems.

4.1. Goal and scope definition

A comparative life cycle assessment (LCA) was performed for producing an aluminum wall by two different additive manufacturing approaches: FSD and CMT-WAAM. The analysis aims to identify the environmental impact characterization of the FSD process in comparison to the established WAAM technology. SimaPro and the Ecoinvent 3 database were utilized to conduct the cradle-to-gate comparative LCA.

4.2. Functional unit and system boundary

The functional unit considered for this study is a wall-shaped component with dimensions of 125 mm× 14 mm x 10 mm (L x W x H). This component is manufactured using the two previously introduced technologies, WAAM and FSD. The authors are aware that the two processes provide the manufactured components with different mechanical properties; however, it is assumed that both products meet the in-use requirements for the produced part.

The system boundaries considered in this study range from the extraction of the raw materials to the production of the functional unit. The recycling is considered as End-Of-Life practice for aluminum alloys, the credit arising from recycling has been included by using the Recycled Content approach [51] with an R (Recycled Content) equal to 45 % and double counting was avoided in accordance with ISO 14040/44.

All the process steps considered for the two different processes are shown in Fig. 6, a. A mass flow study was conducted to assess the starting amount of material needed for the manufacturing of the functional unit. It is worth noting that the FSD method requires an amount of material about 6 times bigger than that required by the CMT-WAAM approach (Fig. 6, b, c).

Since the two parts have the same mass, it is assumed that no difference in the use phase occurs; therefore, this stage was left out of the analysis.

4.3. Life cycle inventory (LCI)

Following Recycled Content approach, the starting ingot reported in Fig. 6 is made of 55 % primary production material and 45 % secondary production material [52].

The secondary production, involving the remelting of scrap, was modeled using data from the European Aluminum Environmental Profile Report [53].

To consider permanent losses due to oxidation during scrap remelting, an extra 16 % of primary aluminum was incorporated [54]. These losses were replaced by adding primary aluminum modeled on SimaPro. The European Aluminum Report [53] was used as source for modeling the Extrusion process, while for the Wire drawing, the CES Edupack database was used [52]. Concerning the machining operations to remove the allowance, both roughing and finishing operations were considered. The SEC models proposed by Kara and Li [45] were used, and two different values of MRR were considered, namely 0.0539 kWh (wall from FSD) and 0.0258 kWh (wall from WAAM) for the roughing and finishing operations, respectively. The processing energy for both FSD and WAAM was experimentally quantified. For the FSD, both deposition and pre-deposition energy values were considered. The energy consumption due to the consumable tool clamping and its dismounting (after the deposition step) was not included in the present analysis. This choice was driven by the lack of industrial practices and of dedicated machines with optimized operations. In Table 2 the detailed information on the CMT-WAAM process inventories is reported. Where experimental data was not available, secondary data from Ecoinvent 3 was employed.

All the analyses were conducted considering Italy's national energy mix in electricity supply.

4.4. Interpretation of the results

To evaluate the environmental impact of the compared processes and to identify the critical issues associated with each technology, an analysis was conducted using the Cumulative Energy Demand (CED) method (Fig. 7a). An additional impact assessment breakdown analysis is provided for depicting the contribution of each factor of influence towards the total CED value (Fig. 7b).

It can be observed that the FSD process has the highest impact in terms of CED. This impact is mainly due to the larger amount of material involved (409 gr vs. 102 gr as shown in Fig. 6). Considering the functional unit weight, the FSD process impact is given by a higher amount of process scrap (undeposited material as shown in Fig. 1) making the highest contribution to the total CED. At the same time, the cumulative energy demand for the pure processing phase accounts for 3.87 % and 34.72 % for the FSD and WAAM processes, respectively. The small impact of the FSD processing step makes the assumption of leaving the non productive time out reasonable. In fact, an inclusion of this contribution would not affect the comparative analysis results significantly.

Also, environmental impact analysis for both FSD and WAAM processes has been performed (Fig. 8).

In Fig. 8, the contribution of each subcategory of impact is shown in milli-points (mPt) based on the Midpoint ReCiPe2016 (H) method. It can be observed from the figure that the Global warming potential, fine particulate matter formation, human carcinogenic and non-carcinogenic toxicity are the categories that mostly affect the mPt metric of both processes.

4.5. Impact of the layer deposition length on the environmental impact

As observed in the previous section, the environmental performance of FSD approach is badly affected by the large amount of process scrap.

Actually, the process is characterized by two different types of scrap. The first type is the flash that progressively grows during the deposition (Fig. 1, c) and the second one is the portion of the consumable rotating tool needed for its clamping (Fig. 1, c). The latter contribution does not vary with changing the deposition lengths and, therefore, its contribution decreases with increasing the lengths of the deposited layer. In order to investigate this phenomenon, environmental impact comparative analyses were carried out for three different deposition lengths: 200 mm, 400 mm and 600 mm; results in terms of CED are reported in Fig. 9. It is possible to note that the difference between the two processes decreases with increasing the layer deposition length. More than that, in the 600 mm case study, the FSD outperforms the WAAM approach by more than 25 %. Such result overturning is basically due to the reduced impact of the material (with respect to the material impact of the WAAM) in the FSD energy breakdown analysis as reported in Fig. 10.

Summing up, with increasing deposition length, the impact of the material needed for the consumable tool clamping is allocated over a larger amount of material, and therefore the unit CED (CED needed for depositing of 1 mm of layer keeping the diameter of the consumable tool unchanged) decreases as the layer deposition length increases.

In Fig. 11 the trend of the specific CED of the two processes is reported, revealing the breakeven point where the two approaches have the same environmental impact.

It is visible that the FSD process can become more environmentally friendly in comparison with WAAM starting from approximately 450 mm of deposit length. It becomes possible because CMT-WAAM processing energy is higher than FSD one, and to build the same functional unit it is necessary to significantly increase the amount of dot-by-dot deposition cycles. In contrast, with increased length, the energy of FSD process remains low, but the material impact decreases if the usage of a unique tool is considered. In Fig. 12 it is shown that for consumable tools, the fraction of material scraps significantly decreases with longer deposition lengths.

It must be noted that there are several real-life examples of WAAMed components such as beams with a total layer length up to 6 m [43]. At the same time, the layer length in FSD case cannot increase infinitely, as it has its own technological limitations connected to process stability. This is caused by the fact that, by increasing the layer length, the tool length should also be increased. Further change of the deposit geometry for more than 600 mm should consider the possibility of using any supporting structures or other ways to keep up the tool position accuracy and deposition quality. Nonetheless, FSD is already overperforming WAAM in environmental impact at the length of 600 mm, so the one layer can possibly be deposited using several tools with no negative effect. Another way to allow the long deposition is to utilize the additive friction stir deposition technique, which has a stationary shoulder and independent axis for the feedstock. More than that, this process also provides reduced process scrap, making this process a serious competitor for both FSD and WAAM, so the analysis of AFSD environmental impact can be considered in future studies.

5. Conclusions

The present study reports the environmental impact characterization of the FSD process along with the comparative analysis with CMT-WAAM approach. Based on the experimental campaign results and the full LCA analysis, the following conclusions have been made.

The most significant effect on the electrical energy during the Friction Surfacing Deposition is provided by the travel speed because of the reduced lead time. The interaction of travel speed with loading force has also sufficient influence, while it is leading to a slight increase of energy. Specific Energy Consumption (SEC) decreases while the deposition rate becomes higher, demonstrating the strong influence of process efficiency on energy consumption.

Environmental impact of FSD technology is badly affected by the larger amount of process scrap while processing energy is lower in comparison with CMT-WAAM. The main contributors to the high material impact of FSD are the flash forming during the processing and the part of the tool needed for clamping.

The outcome of Cumulative Energy Demand comparative analyses of the considered processes is affected by the length of the deposited layer. For short lengths, the CMT-WAAM is the more environmentally friendly choice, while as the length increases, the FSD performance is improving until outperforming the WAAM for lengths bigger than about 450 mm.

Further development of this study will concern the analysis of the environmental impact of AFSD processes with a higher TRL level such as the MELD [25] because of two reasons. First, AFSD processes have no limitations on deposition length because of a special feeding system. Second, these processes are, in fact, characterized by the absence of process scrap (apart from the scrap due to the machining operations).

CRediT authorship contribution statement

Amantia Simone: Data curation, Formal analysis, Investigation, Software, Validation, Writing – original draft. **ingarao Giuseppe:** Conceptualization, Formal analysis, Investigation, Methodology, Supervision, Writing – original draft, Writing – review & editing. **Fratini Livan:** Conceptualization, Project administration, Supervision, Writing – review & editing. **Campatelli Gianni:** Conceptualization, Data curation, Funding acquisition, Resources, Writing – review & editing. **Kalashnikov Kirill:** Data curation, Investigation, Validation, Writing – original draft, Writing – review & editing.

Declaration of Competing Interest

The authors declare that they have no known competing financial interests or personal relationships that could have appeared to influence the work reported in this paper.

Acknowledgements

This study was carried out within the activity of project using Italian MUR funds: “Aluminum Low Impact Circular Economy (ALICE)”, funded by the European Union - Next Generation EU, Mission 4 Component 1, Project: P2022WN727, CUP: B53D23027340001 PRIN 2022-PNRR.

References

[1] Bacciaglia A, Ceruti A, Liverani A. Towards Large Parts Manufacturing in Additive Technologies for Aerospace and Automotive applications. Procedia Comput Sci 2022;200:1113–24. https://doi.org/10.1016/j.procs.2022.01.311.
[2] Routray KL, Saha S. The Economic Impact of Additive Manufacturing Industries. In: Rajendrachari S, editor. Practical Implementations of Additive Manufacturing Technologies. Singapore: Springer Nature Singapore; 2024. p. 309–23. https://doi.org/10.1007/978-981-99-5949-5_15.
[3] Gonçalves A, Ferreira B, Leite M, Ribeiro I. Environmental and Economic Sustainability Impacts of Metal Additive Manufacturing: A Study in the Industrial Machinery and Aeronautical Sectors. Sustain Prod Consum 2023;42:292–308. https://doi.org/10.1016/j.spc.2023.10.004.
[4] Raoufi K, Haapala KR, Etheridge T, Manoharan S, Paul BK. Cost and environmental impact assessment of stainless steel microscale chemical reactor components using conventional and additive manufacturing processes. J Manuf Syst 2022;62:202–17. https://doi.org/10.1016/j.jmsy.2021.11.017.
[5] Seltzman AH, Wukitch SJ. Resolution and geometric limitations in laser powder bed fusion additively manufactured GRCop-84 structures for a lower hybrid current drive launcher. Fusion Eng Des 2021;173:112847. https://doi.org/10.1016/j.fusengdes.2021.112847.
[6] Gao C, Wolff S, Wang S. Eco-friendly additive manufacturing of metals: Energy efficiency and life cycle analysis. J Manuf Syst 2021;60:459–72. https://doi.org/10.1016/j.jmsy.2021.06.011.
[7] Zhao N, Parthasarathy M, Patil S, Coates D, Myers K, Zhu H, et al. Direct additive manufacturing of metal parts for automotive applications. J Manuf Syst 2023;68:368–75. https://doi.org/10.1016/j.jmsy.2023.04.008.
[8] Thompson SM, Bian L, Shamsaei N, Yadollahi A. An overview of Direct Laser Deposition for additive manufacturing; Part I: Transport phenomena, modeling and diagnostics. Addit Manuf 2015;8:36–62. https://doi.org/10.1016/j.addma.2015.07.001.
[9] Filippov AV, Fortuna SV, Gurianov DA, Kalashnikov KN. On the problem of formation of articles with specified properties by the method of electron beam freeform fabrication. J Phys Conf Ser 2018;1115:042044. https://doi.org/10.1088/1742-6596/1115/4/042044.
[10] Li Y, Su C, Zhu J. Comprehensive review of wire arc additive manufacturing: Hardware system, physical process, monitoring, property characterization, application and future prospects. Results Eng 2022;13:100330. https://doi.org/10.1016/j.rineng.2021.100330.
[11] Ostolaza M, Arrizubieta JI, Lamikiz A, Plaza S, Ortega N. Latest Developments to Manufacture Metal Matrix Composites and Functionally Graded Materials through AM: A State-of-the-Art Review. Mater (Basel) 2023;16:1746. https://doi.org/10.3390/ma16041746.
[12] Xia C, Pan Z, Polden J, Li H, Xu Y, Chen S, Zhang Y. A review on wire arc additive manufacturing: Monitoring, control and a framework of automated system. J Manuf Syst 2020;57:31–45. https://doi.org/10.1016/j.jmsy.2020.08.008.
[13] Selvi S, Vishvaksenan A, Rajasekar E. Cold metal transfer (CMT) technology - An overview. Def Technol 2018;14:28–44. https://doi.org/10.1016/j.dt.2017.08.002.
[14] Tomar B, Shiva S. Cold metal transfer-based wire arc additive manufacturing. J Braz Soc Mech Sci Eng 2023;45:157. https://doi.org/10.1007/s40430-023-04084-2.
[15] Gao Q, Lyu F, Wang L, Zhan X. Investigation of Arc Stability in Wire Arc Additive Manufacturing of 2319 Aluminum Alloy. Mater (Basel) 2024;17. https://doi.org/10.3390/ma17215160.
[16] Pan Y, Yu M, Xu C, Zhang J, Geng L. High-Performance 2319 Aluminum Alloy via CMT-WAAM: Microstructure, Porosity, and Mechanical Properties. Met (Basel) 2024;14. https://doi.org/10.3390/met14070797.
[17] Tuncer N, Bose A. Solid-State Metal Additive Manufacturing: A Review. JOM 2020;72:3090–111. https://doi.org/10.1007/s11837-020-04260-y.
[18] Haghshenas M, Gerlich AP. Joining of automotive sheet materials by friction-based welding methods: A review. Eng Sci Technol Int J 2018;21:130–48. https://doi.org/10.1016/j.jestch.2018.02.008.
[19] El-Zathry NE, Akinlabi S, Woo WL, Patel V, Mahamood RM. Friction Stir-Based Techniques: An Overview. Weld World 2024. https://doi.org/10.1007/s40194-024-01847-w.
[20] Kumar M, Gibbons GJ, Das A, Manna I, Tanner D, Kotadia HR. Additive manufacturing of aluminium alloy 2024 by laser powder bed fusion: microstructural evolution, defects and mechanical properties. Rapid Prototyp J 2021;27:1388–97. https://doi.org/10.1108/RPJ-10-2020-0241.
[21] Ridha MH, Alkhazraji SK, Abdullah IT. Investigation of Friction Stir Welding of AA2024-T4 Thin Sheets for Industrial Applications. IOP Conf Ser Mater Sci Eng 2020;881:12074. https://doi.org/10.1088/1757-899X/881/1/012074.
[22] Shao J, Samaei A, Xue T, Xie X, Guo S, Cao J, et al. Additive friction stir deposition of metallic materials: Process, structure and properties. Mater Des 2023;234:112356. https://doi.org/10.1016/j.matdes.2023.112356.
[23] Seidi E, Miller SF, Carlson BE. Friction Surfacing Deposition by Consumable Tools. J Manuf Sci Eng 2021;143. https://doi.org/10.1115/1.4050924.
[24] Guo D, Lam WI, Kwok CT, Chan SLI, Li W, Yang G, et al. A study on formation mechanism of friction-surfaced stainless steel coating via a stop-action method. Surf Coat Technol 2022;441:128511. https://doi.org/10.1016/j.surfcoat.2022.128511.
[25] MELD Manufacturing. “Applications of MELD technology”. Accessed: Nov. 4, 2024. [Online]. Available: 〈https://www.meldmanufacturing.com/applications/〉.
[26] Gandra J, Krohn H, Miranda RM, Vilaça P, Quintino L, dos Santos JF. Friction surfacing—A review. J Mater Process Technol 2014;214:1062–93. https://doi.org/10.1016/j.jmatprotec.2013.12.008.
[27] Liu XM, Zou ZD, Zhang YH, Qu SY, Wang XH. Transferring mechanism of the coating rod in friction surfacing. Surf Coat Technol 2008;202:1889–94. https://doi.org/10.1016/j.surfcoat.2007.08.024.
[28] Antunes Duda E, Kallien Z, da Silva Soares S, Hernandez Schneider T, Ribeiro Piaggio Cardoso H, Vieira Braga Lemos G, et al. Corrosion behavior of multi-layer friction surfaced structure from dissimilar aluminum alloys. Sci Rep 2024;14:9882. https://doi.org/10.1038/s41598-024-60431-w.
[29] Soujon M, Kallien Z, Roos A, Zeller-Plumhoff B, Klusemann B. Fundamental study of multi-track friction surfacing deposits for dissimilar aluminum alloys with application to additive manufacturing. Mater Des 2022;219:110786. https://doi.org/10.1016/j.matdes.2022.110786.
[30] Karmakar S, Swarnkar R, Pal SK. Effect of multi-layer deposition in solid-state friction stir surfacing-based additive manufacturing for fabrication of large-scale metal product. J Mater Process Technol 2023;320:118107. https://doi.org/10.1016/j.jmatprotec.2023.118107.
[31] Kallien Z, Rath L, Roos A, Klusemann B. Application of friction surfacing for solid state additive manufacturing of cylindrical shell structures. Addit Manuf Lett 2024;8:100184. https://doi.org/10.1016/j.addlet.2023.100184.
[32] Jung S, Kara LB, Nie Z, Simpson TW, Whitefoot KS. Is Additive Manufacturing an Environmentally and Economically Preferred Alternative for Mass Production? Environ Sci Technol 2023;57:6373–86. https://doi.org/10.1021/acs.est.2c04927.
[33] Kokare S, Oliveira JP, Santos TG, Godina R. Environmental and economic assessment of a steel wall fabricated by wire-based directed energy deposition. Addit Manuf 2023;61:103316. https://doi.org/10.1016/j.addma.2022.103316.
[34] Nagarajan HP, Haapala KR. Characterizing the influence of resource-energy-exergy factors on the environmental performance of additive manufacturing systems. J Manuf Syst 2018;48:87–96. https://doi.org/10.1016/j.jmsy.2018.06.005.
[35] Kokare S, Oliveira JP, Godina R. Life cycle assessment of additive manufacturing processes: A review. J Manuf Syst 2023;68:536–59. https://doi.org/10.1016/j.jmsy.2023.05.007.
[36] Kokare S, Shen J, Fonseca PP, Lopes JG, Machado CM, Santos TG, et al. Wire arc additive manufacturing of a high-strength low-alloy steel part: environmental impacts, costs, and mechanical properties. Int J Adv Manuf Technol 2024;134:453–75. https://doi.org/10.1007/s00170-024-14144-z.
[37] Liu Z, Zhao Y, Wang Q, Xing H, Sun J. Modeling and Assessment of Carbon Emissions in Additive-Subtractive Integrated Hybrid Manufacturing Based on Energy and Material Analysis. Int J Precis Eng Manuf Technol 2024;11:799–813. https://doi.org/10.1007/s40684-023-00588-3.
[38] Colombini G, Rosa R, Ferrari AM, Defanti S, Bassoli E. Life cycle assessment of lattice structures: Balancing mass saving and productivity. J Clean Prod 2024;445:141390. https://doi.org/10.1016/j.jclepro.2024.141390.
[39] Reis RC, Kokare S, Oliveira JP, Matias JCO, Godina R. Life cycle assessment of metal products: A comparison between wire arc additive manufacturing and CNC milling. Adv Ind Manuf Eng 2023;6:100117. https://doi.org/10.1016/j.aime.2023.100117.

[40] Bekker ACM, Verlinden JC. Life cycle assessment of wire + arc additive manufacturing compared to green sand casting and CNC milling in stainless steel. J Clean Prod 2018;177:438–47. https://doi.org/10.1016/j.jclepro.2017.12.148.
[41] Kokare S, Oliveira JP, Godina R. A LCA and LCC analysis of pure subtractive manufacturing, wire arc additive manufacturing, and selective laser melting approaches. J Manuf Process 2023;101:67–85. https://doi.org/10.1016/j.jmapro.2023.05.102.
[42] Ahmed AA, Nazzal MA, Darras BM, Eltaggaz A, Deiab IM. Comparative sustainability assessment of powder bed fusion and solid-state additive manufacturing processes: The case of direct metal laser sintering versus additive friction stir deposition. Sustain Mater Technol 2024;39:e00858. https://doi.org/10.1016/j.susmat.2024.e00858.
[43] Mishra RS, Yu HZ. Friction Stir Based Solid-State Additive Manufacturing. JOM 2023;75:4182–4. https://doi.org/10.1007/s11837-023-06138-1.
[44] Liu J, Xu Y, Ge Y, Hou Z, Chen S. Wire and arc additive manufacturing of metal components: a review of recent research developments. Int J Adv Manuf Technol 2020;111:149–98. https://doi.org/10.1007/s00170-020-05966-8.
[45] Kara S, Li W. Unit process energy consumption models for material removal processes. CIRP Ann 2011;60:37–40. https://doi.org/10.1016/j.cirp.2011.03.018.
[46] Baffari D, Reynolds AP, Masnata A, Fratini L, Ingarao G. Friction stir extrusion to recycle aluminum alloys scraps: Energy efficiency characterization. J Manuf Process 2019;43:63–9. https://doi.org/10.1016/j.jmapro.2019.03.049.
[47] Lunetto V, Priarone PC, Galati M, Minetola P. On the correlation between process parameters and specific energy consumption in fused deposition modelling. J Manuf Process 2020;56:1039–49. https://doi.org/10.1016/j.jmapro.2020.06.002.
[48] ISO – International Organization for Standardization. ISO 14040:2006, Environmental management – Life cycle assessment – Principles and framework. ISO/TC 207, Subcomittee SC5.2006.
[49] ISO – International Organization for Standardization. ISO 14044:2006, Environmental management — Life cycle assessment — Requirements and guidelines. ISO/TC 207, Subcomittee SC5.2006.
[50] E. C. J. R. C. I. for Environment and Sustainability., International reference life cycle data system (ILCD) handbook general guide for life cycle assessment: provisions and action steps. Publications Office, 2011.
[51] Hammond G., Jones C., Lowrie F., Tse P., Research B.S., Association I., et al. Embodied Carbon: The Inventory of Carbon and Energy (ICE). Building Services Research & Information Association; 2011.
[52] Ansys. "Ansys Granta EduPack". Accessed: Nov 4, 2024. Available: ⟨https://www.ansys.com/it-it/products/materials/granta-edupack⟩.
[53] European Aluminum. "Environmental Profile Report 2018". Accessed: Nov 4, 2024. [Online] Available: ⟨https://www.european-a luminium.eu/resource-hub/environmental-profilereport-2018/⟩.
[54] Duflou JR, Tekkaya AE, Haase M, Welo T, Vanmeensel K, Kellens K, et al. Environmental assessment of solid state recycling routes for aluminium alloys: Can solid state processes significantly reduce the environmental impact of aluminium recycling? CIRP Ann 2015;64:37–40. https://doi.org/10.1016/J.CIRP.2015.04.051.